# Runaway Electron Confinement Modeling
# for DIII-D, Alcator C-Mod and ITER

V.A. Izzo 1), A.N. James 1), E.M. Hollmann 1), J.H. Yu 1), D.A. Humphreys 2),
J.C. Wesley 2), L.L. Lao 2), P.B. Parks 2), P.E. Sieck 2), D.G. Whyte 3), G.M. Olynyk 3),
and R.S. Granetz 3)

1) University of California-San Diego, 9500 Gilman Dr., La Jolla, California 92093, USA
2) General Atomics, PO Box 95608, San Diego, California 92186-5608, USA
3) Massachusetts Institute of Technology, Cambridge, Massachusetts 02139, USA

Contact email for first author: izzo@fusion.gat.com

**Abstract.** Nonlinear MHD simulations of rapid shutdowns (or disruptions) in three tokamaks — DIII-D, Alcator C-Mod, and ITER — are performed with the NIMROD code. The simulation are initiated by depositing a large amount of neutral Ar in the plasma to initiate a radiative thermal quench, which modifies the current profile and leads to the onset of MHD instability. During the simulations, drift-orbits for a trace population of runaway electrons are integrated, in order to study the interaction between disruption-induced MHD and runaway electron confinement. DIII-D simulations show significantly greater runaway electron transport in diverted plasma disruptions that in limited plasma disruptions. In C-Mod, an edge-peaked [massive gas injection (MGI)-like] fueling profile is found to delay the loss of core confined runaway electrons relative to core-peaked (pellet-like) profile, although all runaway electrons are eventually lost in both cases. A comparison of results across all three devices suggests a strong reduction in runaway electron transport with increasing machine size, which is an unfavorable result for ITER.

## 1. Introduction

During tokamak disruptions, large electric fields can produce high-energy runaway electrons (RE), whose population grows exponentially during the current quench (CQ) due to the knock-on avalanche phenomenon [1]. In practice, the runaway avalanche competes with other processes such as collisional slowing or transport losses of REs, producing a wide variability of runaway conversion across different tokamaks, plasma shapes, and disruption types. The total avalanche gain (multiplication factor relative to the seed population) during the CQ depends on the exponential of the initial plasma current ($G_{RE} \approx \exp[2.5 \, I_p \, (MA)]$ [2]). This relationship demands extrapolation of 10 or more orders of magnitude from tokamaks having a few MA of plasma current to ITER (~15 MA). The threat posed by RE to the ITER first wall is therefore difficult to assess experimentally, and well-validated models are required to investigate the high-gain regime. In this paper we focus not on avalanche growth, but on modeling transport losses of REs due to disruption related MHD fluctuations. If the loss rate of REs exceeds the avalanche growth rate, no significant RE conversion should occur. Thus it is desirable to understand what factors produce the largest RE loss rate (for the largest fraction of the CQ time), and how RE transport can be enhanced in the CQ phase of disruption. Here we investigate how both the pre-disruption plasma configuration (limited vs. diverted) and the means of disruption mitigation (gas-jet vs. pellet) will impact the resulting MHD fluctuations and RE transport losses.

## 2. Model

In this paper we perform extended-MHD simulations with the NIMROD code [3]. The resistive MHD model used evolves the magnetic field, a single fluid velocity, a single temperature and a set of continuity equations governing the deuterium ion density, and the

density of each charge state (including neutrals) of an impurity species, in this case argon. The inclusion of an impurity species allows rapid shutdown techniques based on massive particle injection (MPI) to be modeled (including gas injection, pellet injection, etc). Cooling due to ionization, radiation, and recombination is incorporated into the temperature evolution. To initiate an MPI shutdown simulation, a source of neutral impurity atoms is specified. The impurity source can entail a gradual delivery of atoms, or an instantaneous delivery, in which all of the injected atoms are deposited with a prescribed spatial distribution at $t$=0. The latter method, while less physically realistic, can greatly reduce computational intensiveness of the simulation, and is thus used in the simulations described in the following sections.

A test-particle orbit-tracing module computes the transport of REs as the MHD fields evolve. This module advances the guiding-center drift orbits of a collection of trace REs after each MHD time-step, using the updated magnetic and electric fields. The test REs are initiated with random positions and specified energies above the runaway threshold. Four equations governing three spatial coordinates [$R,Z,\phi$] and parallel velocity are integrated. The velocity equation includes acceleration by the electric field and slowing terms due to collisions, synchrotron and bremsstrahlung radiation. The component of velocity normal to the magnetic field (used in the synchrotron calculation) is assumed based on a fixed pitch angle of 0.1.

## 3. DIII-D Simulations

In DIII-D, a large number of RE experiments have been initiated by injecting an Ar pellet. The NIMROD simulations are initiated with a quantity of neutral Ar comparable to the experimental pellet mass distributed broadly over the plasma cross-section — the time scale for pellet penetration and ablation is neglected. The instantaneous delivery and non-local deposition produces a very rapid (~0.01 ms) radiative collapse of the plasma temperature, effectively compressing the thermal quench (TQ) time-scale. But, because the plasma temperature quickly drops from the keV range to tens of eV (typical of a CQ plasma), the typical numerical difficulties (wide time-scale separation) associated with simulating a high-performance tokamak plasma are avoided. In particular, the CQ phase can be simulated with a realistic (Spitzer) value of resistivity and proceeds on the correct, physical time-scale. The cool, resistive CQ phase is also well described by the resistive MHD model.

The initial equilibria for two DIII-D simulations appear in Fig. 1, along with the starting [$R,Z$] positions for the 1598 REs whose orbits are traced. The first equilibrium (DIII-D shot 137611) is a lower single null (LSN) diverted discharge,
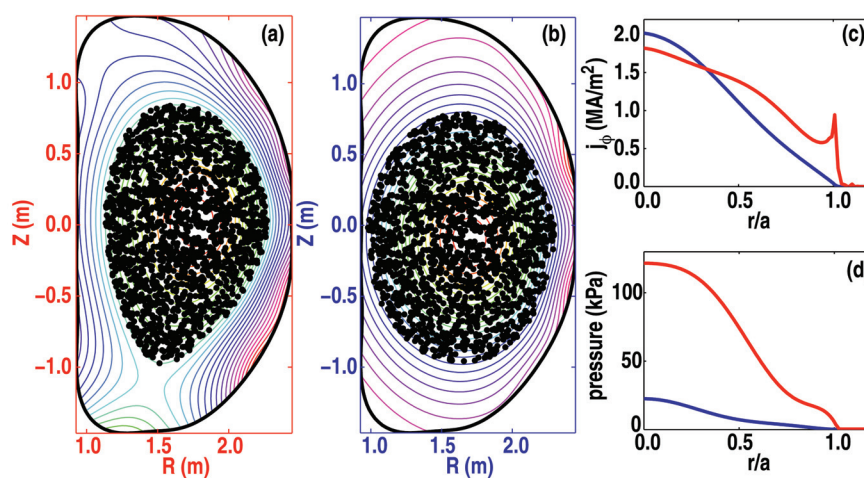


FIG. 1. *Poloidal flux contours for the diverted (left) and limited (center) DIII-D simulations, with starting locations for 1598 REs superimposed. (Right) Toroidal current density and plasma pressure profiles for the two equilibria.*

whereas the second (shot 140586) is an inner-wall-limited equilibrium. Experimentally, both of these discharges produced significant RE current plateaus following an Ar pellet-triggered rapid shutdown. However, in general, limited DIII-D plasma shapes produce RE current plateaus with much greater reliability (over a series of repeat discharges) than do diverted plasma shapes. The role of MHD-induced RE losses in that experimental trend is investigated by this pair of simulations.

Both DIII-D simulations have approximately 3 ms current quench times, which is comparable to DIII-D experiments. In the diverted simulation (Fig. 2), the core temperature initially drops to 30 eV, where the radiation and ohmic heating approximately balance until the onset of MHD at around 0.6 ms. The MHD is triggered by the peaking of the current channel. As the core temperature then drops



FIG. 2. Time histories of (a) total plasma current, (b) total number of confined REs, (c) loss rate of REs, and (d) n=1,2, and 3 magnetic fluctuation amplitude. (e) Field line puncture plot at 0.8 ms. Red X is approximate striking location of all REs lost at this time.

further to 10 eV, 32% of the seed RE population is lost as a result of MHD activity (near 0.8 ms). All of these escaping REs impact the outer divertor strikepoint in a poloidally localized, but toroidally symmetric pattern, with a characteristic loss time of 0.25 ms. The first set of MHD modes to appear are $n=1, 2$, and 3 modes of similar amplitude. These are all $q=1$ modes, but have no effect on the RE confinement. The second MHD event, which is responsible for the RE losses, is dominanted by the $n=2$ mode, comprising both 3/2 and 2/2 components. Late in time (near 2 ms), REs begin to escape due to the decay of the confining plasma current, and strike the outer-midplane. Since the current carried by the trace REs is neglected, the physical model becomes inaccurate in this late stage of the CQ, when the RE current would be comparable to the plasma current.

In the simulation of limited DIII-D discharge 140586, the onset of MHD occurs at nearly the same time as in the diverted case, but exhibits a somewhat different character. The first set of $q=1$ modes to appear do not result in RE deconfinement, just as in the diverted case, although in the limited simulation, the stochasticity associated with these modes is entirely localized to the core region, leaving the outer flux surfaces intact. This degree of localization is not seen in the diverted simulation. The MHD event that is associated with RE losses in this case is nearly a pure $n=1$ mode, with m numbers ranging from 2–6. A corresponding series of distinct $n=1$ islands is present when this mode reaches saturation, but there is no clear connection from field lines in the core to those in the edge. Indeed, the loss of REs in this simulation appears not to be primarily associated with transport on stochastic field lines, but rather with an external $n=1$ shift of the plasma into the center column, causing REs with large
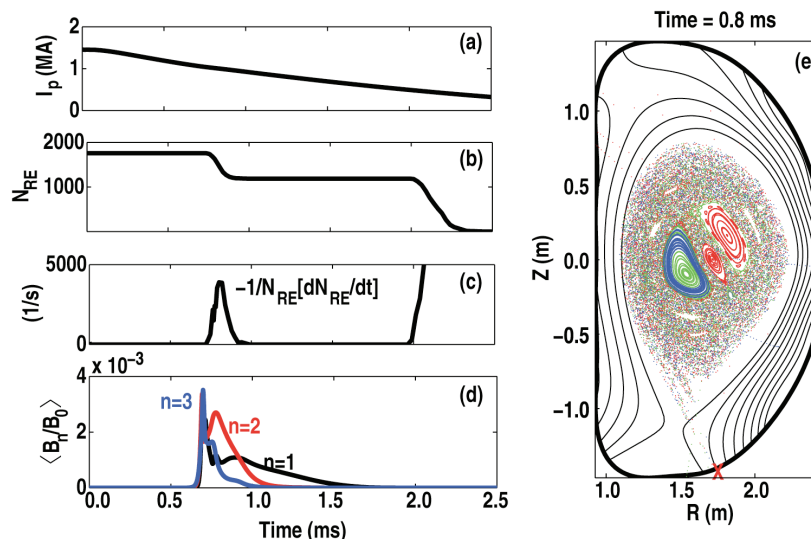
minor radius to impact the center column with a characteristic $n$=1 striking pattern. Only 11% of the initial RE population is lost as a result of the $n$=1 mode.

The RE loss pattern associated with the $n$=1 mode in the limited simulation appears in the left column of Fig. 3. The characteristic loss time for REs in this simulation is 2 ms, or several times longer than the diverted simulation. An initial $n$=1 localized burst of REs strikes the center column during the late growth phase of the secondary $n$=1 mode. Beginning at the time of mode saturation, a toroidally propagating $n$=1 striking pattern of REs on the center column is seen. These results can be compared directly to observation of hard x-rays (HXR) seen in DIII-D shot 140586. A set of five HXR scintillators is located outside the DIII-D vessel at the midplane. These scintillators detect HXR signals produced when high energy REs impact the material wall. An initial localized burst is seen, peaked on the 155° detector about 3.5 ms after pellet injection. Subsequently, a lower level toroidally propagating $n$=1 signal is seen. Magnetic probe data at the outer midplane indicates a larger amplitude $n$=1 mode before the HXR signals appear, and a lower amplitude, but toroidally propagating $n$=1 mode at the time of the HXR signals.
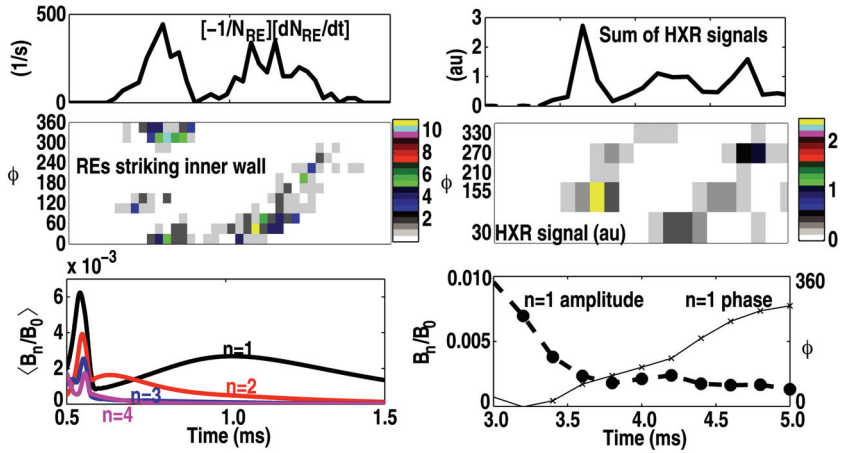


FIG. 3. (Left) NIMROD simulation of shot 140586 showing: (top) total loss rate of REs; (middle) number of REs striking the inner midplane at a given time and toroidal angle; and (bottom) Amplitude of $n$=1–4 modes divided by $n$=0 amplitude. (Right) Data from DIII-D shot 140586 showing: (top) Sum of all midplane hard x-ray detectors vs. time; (middle) HXR signals at five toroidal angles vs. time; and (bottom) measured amplitude and phase of $n$=1 magnetic fluctuations at outer midplane.

## 4. Alcator C-Mod Simulations

In Alcator C-Mod, runaway electron experiments have been carried out using massive gas injection (MGI) as a means of rapid shutdown [4]. In these experiments, lower hybrid current drive (LHCD) is used to produce a large seed population of REs before the gas jet is triggered. For diverted geometry plasmas, all REs appear to be deconfined in the TQ phase, with no avalanche growth observed in the CQ.

The two C-Mod simulations presented here differ significantly from MGI experiments in which nearly all of the neutral Ar is initially in the edge, due to poor penetration of the gas jet. Here, we seek to make connections between similar shutdown scenarios on different machines, so we begin with a simulation having a core peaked Ar profile comparable to the DIII-D simulations. Then, to explore the effects of fueling profile, we run a second simulation with an edge-peaked profile, but nearly the same total Ar quantity. Note that the second simulation still has much more Ar in the core and much less in the edge than the pre-TQ conditions for an actual C-Mod MGI experiment. The initial conditions for the two

simulations appear in Figs. 4(a) and 4(b). Figure 4(b) also shows the Ar profile at the end of the simulation (1.3 ms) for the initially edge-peaked case, showing considerable flattening/mixing of the Ar. In Figs. 4(c,d) are the temperature and current density profiles at 0.1 ms, before the onset of MHD in either case. As expected, the core-peaked profile produces faster cooling of the core as well was faster contraction of the current profile. The time evolution of the total plasma current and the total number of confined REs are seen in Fig. 4(e,f).
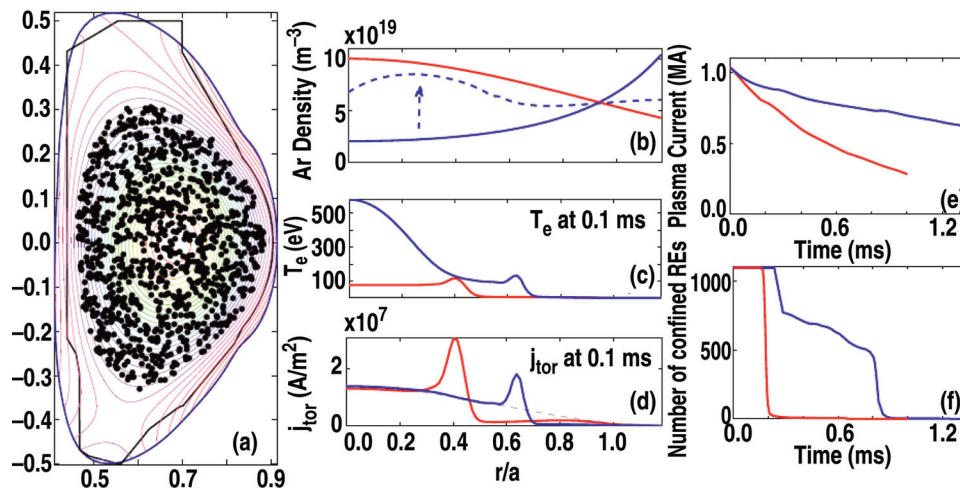


FIG. 4. (a) C-Mod wall shape (black line), simulation boundary (blue line), starting (r,z) locations of 1098 REs (black dots), and initial poloidal flux contours. (b) Initial neutral Ar profiles for the two C-Mod simulations (solid), and the final Ar (ions + neutrals) profile for the initially edge-peaked case. Profiles of (c) $T_e$ and (d) $j_\phi$ at t = 0.1 ms for both cases. And, time histories for each case of (e) plasma current decay, (f) total number of confine REs.

A notable feature of the C-Mod simulations is that in both cases the number of confined runaway electrons goes to zero when an appreciable fraction of the plasma current remains. In the core-peaked simulation, nearly all of the electrons are lost in a single event at 0.2 ms, whereas the edge-peaked case, they are primarily lost in two discreet events, the second of which (0.9 ms) is concurrent with a very slight increase in total plasma current. As in the DIII-D diverted simulation, all of the RE losses are localized to the outer-divertor strike point and the outer midplane, just above Z=0. In each case, an initial RE loss event occurs near the time of saturation of the initial unstable MHD mode, as seen in Fig. 5. In the core-peaked simulation, $n=2$ (2/2 +3/2) and $n=1$ (1/1 + 2/1) modes saturate at nearly the same time, with the $n=2$ dominant. The RE loss pattern on the outer-midplane exhibits a combination of $n=1$ and $n=2$ symmetry, while RE losses to the outer divertor are predominantly $n=0$. Likewise, the initial striking pattern in the edge peaked simulation exhibits the $n=3$ symmetry of the dominant mode (4/3) at the midplane and $n=0$ symmetry at the divertor. In that case, the larger RE loss event is associated with an $n=1$ mode just after 0.8 ms. That $n=1$ mode is also primarily responsible for the core density increase seen in Fig. 4(b) — the core Ar density remains roughly constant until that time. During the fastest RE loss events, these two simulations have characteristic RE loss times of around 10 μs and 25 μs respectively, as seen in the top row of Fig. 5.
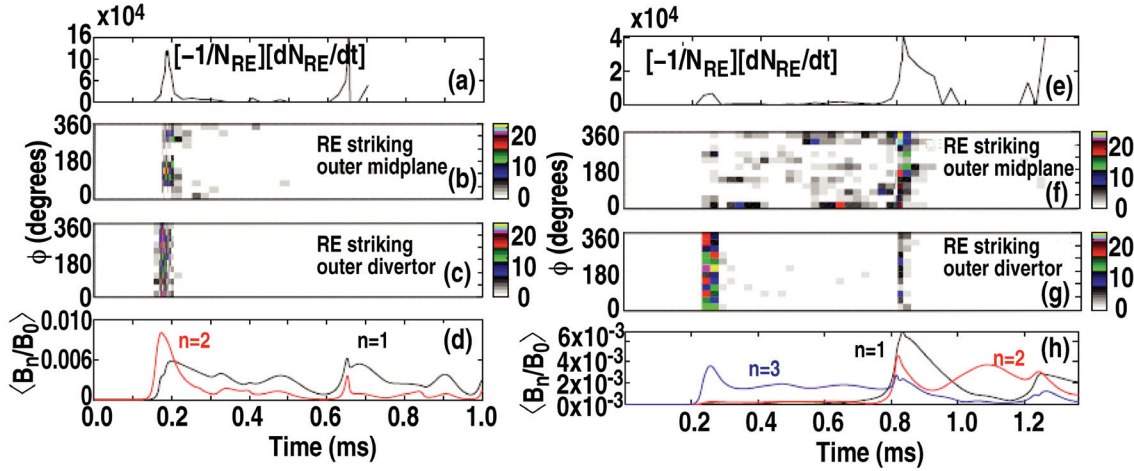
FIG. 5. (Left) Core-peaked simulation. (Right) Edge peaked simulation. (Top to bottom) Total loss rate of REs (1/s), 2D histograms of RE losses vs. time and toroidal angle at the outer mid-plane and outer divertor, and MHD mode amplitudes divided by n=0 amplitude.

## 5. ITER Simulation

One ITER simulation is performed with a diverted plasma geometry (Fig. 6) and a core-peaked neutral Ar profile that can be compared directly to the similar simulations performed for both C-Mod and DIII-D. In the ITER simulation, only toroidal mode numbers $n$=0–5 are included (due to limited computational resources), unlike the C-Mod and DIII-D cases having $n$=0–10. The same Spitzer resistivity expression is used in this simulation as for the other tokamaks, with the caveat that the maximum temperature used in the evaluation of the resistivity is set to 300 eV (only in the Ohm's law —not for Ohmic heating). Once the plasma temperature is below 300 eV everywhere, the resistivity is identical to Spitzer.

The ITER simulation is carried out for 5.5 ms, at which point about 2/3 of the initial current remains (Fig. 6). The onset of MHD occurs about 1 ms into the simulation, and is dominated by an $n$=1 mode (1/1). The magnitude of the fluctuating fields relative to the equilibrium is quite comparable to the other simulations. However, in the ITER case, no REs are deconfined by MHD activity. Beginning shortly after 2 ms, REs at large minor radius begin to escape due to the shrinking equilibrium as the plasma current decays. These electrons hit the wall at the outer divertor strikepoint.
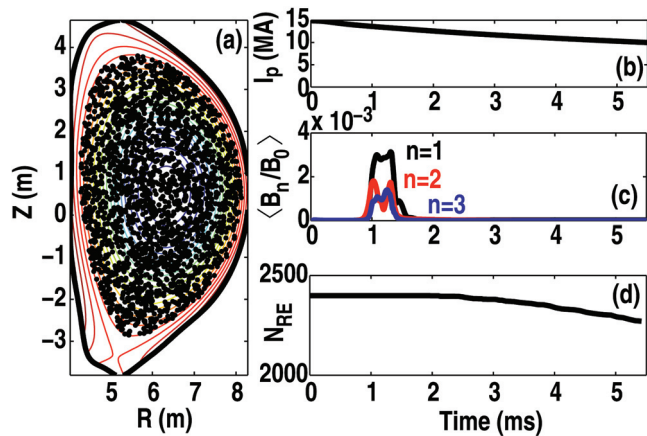


FIG. 6. (Left) ITER simulation geometry with 2399 RE orbit starting point marked. (Right) Time histories of (top) total plasma current, (middle) fluctuating field amplitudes, and (bottom) total number of confined REs.

Field line traces from the times associated with each of the two peaks in the $n$=2 mode amplitude are shown in Fig. 7. At each time, considerable stochasticity in the core is surrounded by a region of unperturbed flux surfaces. Also shown in Fig. 7 are the

temperature and current density profiles at the same two times. At 1.05 ms, the temperature remains above 300 eV inside of about $r/a$=0.4, meaning that the resistivity is still artificially enhanced in this region. However, by 1.3 ms, the resistivity is Spitzer or very close to Spitzer across the entire domain, as the peak temperature has dropped to nearly 300 eV.
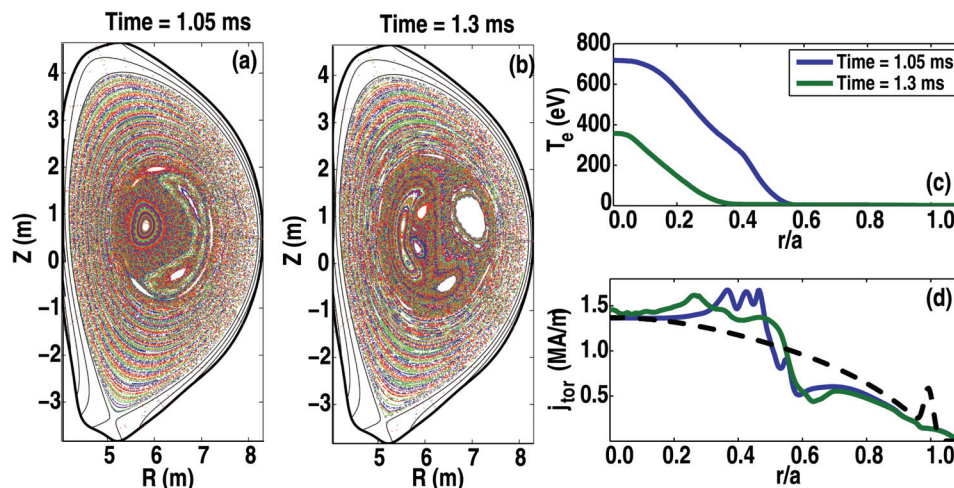
FIG. 7. (Left) Field line puncture plots at two times corresponding to two peaks in the n=1 mode amplitude. (Right) Profiles of $T_e$ (top) and $j_\phi$ (bottom) at the same two times (dashed line is initial current density profile).

## 6. Discussion and Conclusions

We have performed simulations of three tokamaks — Alcator C-Mod, DIII-D and ITER — undergoing a rapid shutdown due to a radiative collapse following the introduction of a large quantity of Ar. By following drift orbits for a trace population of REs we have obtained information on confinement of REs during the TQ-induced MHD perturbations in each device. In a cross-device comparison, the most significant qualitative observation we can make is that in the smallest device (C-Mod) all of the REs were deconfined by MHD fluctuations, in the largest device (ITER) none of the REs were deconfined, and in the intermediate sized device (DIII-D) a fraction of the REs were deconfined. This immediately suggests an unfavorable scaling of the RE losses during disruptions with device major radius, since REs that remain confined can accelerate to higher energies and grow exponentially in number, producing a more catastrophic loss to the wall late in time. From an examination of the flux surfaces, it is clear why REs in the ITER simulation remained confined. In each of the smaller devices, stochasticity extends to the separatrix. But, at comparable magnetic fluctuation levels, the RE loss rate differs considerably in these two devices. If we compare just the two most similar simulations — those with diverted geometry and core-peaked Ar profiles — the characteristic loss time for an RE in DIII-D is about 25 times that in C-Mod, which is a factor of $R^3$ (Fig. 8). This scaling would suggest a loss time for ITER of 10 ms even if the stochasticity extended to the boundary. For an appreciable fraction of REs to be lost, we would expect that the duration of the MHD fluctuations would need to be an appreciable fraction of this time, which is quite long compared to the 0.5 ms duration in the ITER simulation.

The major limitation of these simulations is the simplifying assumption of instantaneous Ar delivery, which is made for reasons of numerical expediency. More accurate Ar delivery models might alter the nature of the MHD fluctuations and hence the RE losses. In particular we note that the edge-peaked Ar profile used for one C-Mod simulation is still quite dissimilar from MGI, so further studies are required to understand RE confinement in an MGI case where the core $T_e$ remains very high until the onset of MHD. In MGI experiments, as in many "natural" disruptions, a current spike (increase in $I_p$) is typically observed at the start of the CQ phase. This contrasts
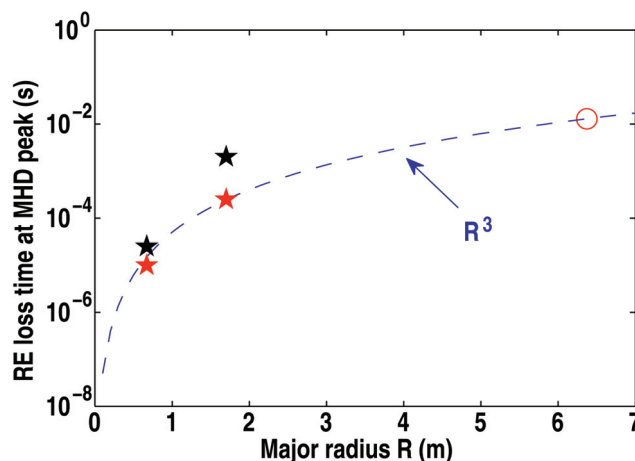
FIG. 8. Characteristic loss time for REs in all simulations of C-Mod and DIII-D. Red stars are the two most similar cases —diverted geometry and core-peaked Ar. The dashed blue line is proportional to $R^3$. The red circle indicates where ITER would fall on that curve.

with DIII-D Ar pellet experiments where no current spike is generally seen. Note that in the edge-peaked C-Mod simulation a small increase in total $I_p$ is seen just before 1 ms (at the time of the 1/1 mode), whereas no such increase is seen in the other simulations. The lower core resistivity may be a key factor in the presence of a current spike for MGI.

The experimental observation in DIII-D that limited discharges confine REs more reliably than diverted discharges can be understood in light of the two DIII-D simulations presented here. The RE losses in the diverted geometry are due to stochastic fields extending across the domain, whereas the RE losses seen in the limited geometry are associated with $n=1$ plasma motion into the center column, and not transport on stochastic fields. Comparison with DIII-D HXR data supports the possibility that the same loss mechanism occurs in the experiments. Further simulations are required to understand the difference between diverted plasmas that do and do not produce RE plateaus.

**References**

[1] JAYAKUMAR, R., *et al.,* Phys. Lett. **A 172** (1993) 447
[2] ITER Physics Expert Group on Disruptions, Plasma Control, and MHD, *et al.,* Nucl. Fusion **39** (1999) 2346
[3] SOVINEC, C.R., *et al*., J. Comput. Phys. **195** (2004) 355
[4] MARMAR, E., *et al.,* Nucl. Fusion **49** (2009) 104014